Biophysical Journal Volume 69 October 1995 1584–1595

Physical and Chemical Effects of Red Cells in the Shear-Induced Aggregation of Human Platelets

Harry L. Goldsmith, David N. Bell, Susan Braovac, Andrew Steinberg, and Fiona McIntosh
McGill University Medical Clinic, Montreal General Hospital, and the Department of Medicine, McGill University, Montreal, Canada

ABSTRACT Both chemical and physical effects of red cells have been implicated in the spontaneous aggregation of platelets in sheared whole blood (WB). To determine whether the chemical effect is due to ADP leaking from the red cells, a previously described technique for measuring the concentration and size of single platelets and aggregates was used to study the shear-induced aggregation of platelets in WB flowing through 1.19-mm-diameter polyethylene tubing in the presence and absence of the ADP scavenger enzyme system phosphocreatine-creatine phosphokinase (CP-CPK). Significant spontaneous aggregation was observed at mean tube shear rates, $\langle G \rangle$ = 41.9 and 335 s^{-1} (42% and 13% decrease in single platelets after a mean transit time $\langle t \rangle$ = 43 s, compared to 89 and 95% decrease with 0.2 μM ADP). The addition of CP-CPK, either at the time of, or 30 min before each run, completely abolished aggregation. In the presence of 0.2 μM ADP, CP-CPK caused a reversal of aggregation at $\langle t \rangle$ = 17 s after 30% of single cells had aggregated. To determine whether red cells exert a physical effect by increasing the time of interaction of two colliding platelets (thereby increasing the proportion of collisions resulting in the formation of aggregates), an optically transparent suspension of 40% reconstituted red cell ghosts in serum containing 2.5-μm-diameter latex spheres ($3 \times 10^5/\mu l$) flowing through 100-μm-diameter tubes was used as a model of platelets in blood, and the results were compared with those obtained in a control suspension of latex spheres in serum alone. Two-body collisions between microspheres in the interior of the flowing ghost cell or serum suspensions at shear rates from 5 to 90 s^{-1} were recorded on cine film. The films were subsequently analyzed, and the measured doublet lifetime, τ_{meas}, was compared with that predicted by theory in the absence of interactions with other particles, τ_{theor}. The mean $\langle \tau_{meas}/\tau_{theor} \rangle$ for doublets in ghost cell suspensions was 1.614 ± 1.795 (SD; n = 320), compared to a value of 1.001 ± 0.312 (n = 90) for doublets in serum. Whereas 11% of doublets in ghost cell suspensions had lifetimes from 2.5 to 5 times greater than predicted, in serum, no doublets had lifetimes greater than 1.91 times that predicted. There was no statistically significant correlation between τ_{meas}/τ_{theor} and shear rate, but the values of τ_{meas}/τ_{theor} for low-angle collisions in ghost cell suspensions were significantly greater than for high-angle collisions.

INTRODUCTION

We have previously reported on the effect of red blood cells (rbc) in increasing both the rate and extent of ADP-induced aggregation of human platelets flowing through small tubes (Bell et al., 1990). By means of a double infusion technique, whole blood (WB) and agonist were rapidly mixed in a small chamber, and then flowed through tubes for various times at mean shear rates $\langle G \rangle$ from 42 to 1920 s^{-1}. The reaction was quenched in glutaraldehyde; single platelets and aggregates were separated from red cells and then counted in a resistive particle counter. It was found that the initial rate of aggregation, as measured by the disappearance of single platelets, was up to 9 times greater than in platelet-rich plasma (PRP). An explanation was sought in terms of the influence of the red cells on the motions and distributions of platelets in blood, in particular the continual shear-induced collisions between rbc which leads to a marked lateral dispersion of platelets (Goldsmith, 1971), resulting in an effective translational diffusion coefficient from 2 to 3 orders of magnitude greater than in PRP (Turitto et al., 1972; Goldsmith and Marlow, 1979). At first, it was thought that higher platelet-platelet collision frequencies due to the enhanced cell diffusion contributed to the higher platelet aggregation in whole blood. However, comparison of the estimated two-body collision frequency due to random Brownian motion enhanced by the red cells, with the two-body shear-induced collision frequency, showed that only at the lowest mean tube shear rate (42 s^{-1}) would there be a significant increase in collision frequency (2.56 times), still much lower than the observed initial increase in the rate of single platelet aggregation (Bell et al., 1990). An alternative explanation was therefore sought in terms of an increased collision efficiency, defined as the ratio of the number of two-body platelet collisions per second per unit volume of suspension resulting in capture (formation of an aggregate) to the total number of two-body collisions/s/unit volume. Such an increased collision efficiency might result from an increased velocity of approach and time of interaction of two platelets during collision, due to the presence of the red cells. One of the aims of the present work was therefore to study two-body collisions in the tube flow of a concentrated suspension to test this hypothesis. To this end, we used an optically transparent suspension of reconstituted red cell ghosts in plasma (Goldsmith, 1971; Goldsmith and Marlow, 1979) containing 2.5-μm-diameter latex spheres as models of platelets flowing through 100-μm-diameter tubes. Shear-

Received for publication 26 September 1994 and in final form 11 July 1995.

Address reprint requests to Dr. Harry L. Goldsmith, University Medical Clinic, Montreal General Hospital, 1650 Cedar Ave., Montreal, Quebec H3G 1A4 Canada. Tel.: 514-937-6011 X2920; Fax: 514-937-6961; E-mail: mdhg@musica.mcgill.ca.

0006-3495/95/10/1584/12 $2.00

induced two-body collisions between microspheres at known local shear rates were viewed in the interior of the ghost cell suspension, captured, and analyzed on cine film.

In addition to the physical effect of the red cells on platelet motions and aggregation, it has been postulated that locally released ADP from rbc is responsible for the observed aggregation in sheared whole blood in the absence of added agonist. There is evidence in vitro that spontaneous platelet aggregation in blood (Fox et al., 1982; Saniabadi et al., 1984, 1985, 1987, 1989; Armstrong et al., 1995), as well as shear-induced platelet aggregation (Jen and McIntire, 1984), is inhibited by enzymes that degrade ADP. It has also been reported that rbc promote the aggregation of platelets activated by exogenous ADP through the uptake of the platelet inhibitor, adenosine (Skoza et al., 1967), which is formed after successive dephosphorylation of adenine nucleotides by enzymes located on the external surface of rbc (Parker, 1970). Thus, it is observed that adenosine is a more potent inhibitor of ADP-induced platelet aggregation in PRP than in WB (Gresele et al., 1986), and that dipyridamole, at concentrations that do not directly inhibit platelets but which block adenosine uptake by rbc (Harker and Kadatz, 1983), inhibits ADP-induced aggregation in WB but not in PRP (Gresele et al., 1983, 1986).

Indeed, our previously reported work with whole blood showed that, in control experiments in which Tyrodes instead of ADP was infused with whole blood into the mixing chamber, there was significant "spontaneous" aggregation at $\langle G \rangle = 42\ s^{-1}$. Such aggregation was much reduced at $\langle G \rangle = 335\ s^{-1}$, but reappeared to a lesser extent at $\langle G \rangle = 1{,}920\ s^{-1}$, where it may have been due to platelet activation because the shear stress, $\sim 6\ Nm^{-2}$, was close to the critical value for shear-induced release (Bell et al., 1990; Dewitz et al., 1978; Jen and McIntire, 1984). The other aim of the present work was therefore to test the chemical role of rbc on platelet aggregation, by testing the effect of the ADP scavenger enzyme system phosphocreatine-creatine phosphokinase (CP-CPK) on spontaneous as well as ADP-induced platelet aggregation in whole blood.

MATERIALS AND METHODS

Whole blood and reagents

Experiments were performed as described in the previous paper on platelet aggregation in whole blood (Bell et al., 1990). Venous blood was slowly drawn from healthy volunteers via a 19-gauge needle and winged infusion set into a 60-ml plastic syringe containing 1/10 volume sodium citrate. Hematocrit was predetermined on undiluted venous blood drawn using the same technique. All donors had refrained from aspirin ingestion for at least 10 days prior to blood withdrawal, and no female donors were taking oral contraceptives. The blood was transferred to polycarbonate tubes, tightly capped, and left to stand at room temperature for 30 min with or without incubation with the enzyme, and the runs were then undertaken. Platelet-poor plasma (PPP) was prepared by centrifugation of a portion of the drawn blood for 10 min at $1000 \times g$.

Solutions of the enzyme system CP-CPK were made up in PPP and added to whole blood to give a final concentration of 0.108 M phosphocreatine and 720 units/ml creatine phosphokinase (Sigma, St. Louis, MO) in the plasma compartment whose volume was known from the measured hematocrit. Tests in the aggregometer showed that, at this concentration of CP-CPK, aggregation of citrated PRP (3×10^5 cells/μl) with 1 μM ADP at 23°C was totally inhibited.

Frozen aliquots of 2 mM adenosine-5′-diphosphate, ADP (Sigma, St. Louis, MO) in modified Tyrodes solution (137 mM NaCl, 2.7 mM KCl, 11.9 mM $NaHCO_3$, 0.36 mM $NaH_2PO_4 \cdot H_2O$) were thawed immediately prior to use. Electron microscope grade glutaraldehyde (J.B. EM Services, Pointe Claire-Dorval, Québec) was diluted to 0.5% (v/v) in Isoton II (Coulter Electronics, Hialeah, FL). One percent (v/v) silicone (Siliclad, Clay Adams, Parsippany, NJ) was used to siliconize the mixing chamber.

Latex spheres and red cell ghosts

Five hundred microliters of an aqueous suspension of 2.5-μm-diameter sulfated polystyrene latex spheres ($7 \times 10^6/\mu$l; Interfacial Dynamics Corporation, Portland, OR) were added to a 40-ml aqueous solution of polyethylene oxide (PEO; molecular mass, $= 10^6$ Da), and stirred for 6 h. The resulting PEO-coated spheres were resistant to aggregation in both physiological saline and plasma.

Suspensions of red cell ghosts, transparent to transmitted light under the microscope, were prepared by sudden osmotic lysis with hypotonic phosphate buffer, and the cells were reconstituted by restoring the normal ionic strength of plasma and resuspended in serum (the latter obtained from the supernatant of 10 ml of blood allowed to clot in a glass tube), as described by Goldsmith and Marlow (1979). The volume concentration of ghost cells was determined by adding 10 μl of ^{125}I-labeled human serum albumin (100 μCi/ml) to a suspension of 500 μl of packed ghost cells diluted with 500 μl serum, and comparing the activity in an aliquot of suspension with that in the cell-free serum. To obtain cell-free serum, some of the suspension was transferred into microhematocrit tubes and centrifuged at $11{,}000 \times g$ for 1 h at 4°C. Twenty-microliter samples of each of the lower serum and upper ghost layers were taken off, and the activity in each was compared with that of the original suspension. Measurements showed that the volume concentration in the original packed ghost cell suspensions varied from 60% to 70% and that the ghost cell layer in the microhematocrit tubes contained between 8% and 15% trapped serum. Suspensions of 40% by volume of ghost cells were prepared by dilution with serum, and PEO-coated latex spheres were added at a final concentration of $3 \times 10^5\ \mu l^{-1}$. For the control experiments, PEO-coated latex spheres were added to serum at a concentration of $3 \times 10^5\ \mu l^{-1}$.

Flow system for platelet aggregation

All experiments were done at 23 ± 1°C. Whole blood and ADP, or whole blood and Tyrodes (in the control runs) flowing from independent infusion pumps (Harvard Apparatus, Bedford, MA) were rapidly mixed in a stirred chamber of 50 μl volume at a fixed flow ratio, WB:ADP or Tyrodes = 9:1 (Bell et al., 1989a). The suspensions flowed out into 2- to 800-cm lengths of polyethylene tubing (Clay Adams, Parsippany, NJ) of radius $R_o = 0.595$ mm, at volume flow rates, Q, of 13 and 104 $\mu l\ s^{-1}$, corresponding to tube Reynolds numbers of ~2.8 and 22, and volume-averaged mean tube shear rates $\langle G \rangle = 32Q/15\pi R_o^3$ (Bell et al., 1989a) of 41.9 and 335 s^{-1}, respectively, assuming Poiseuille flow. The mean transit times, $\langle t \rangle = X/\langle U \rangle$ (X is the distance of flow along the tube and $\langle U \rangle$ the mean linear fluid velocity) ranged from <0.1 to 86 s.

The aggregation reaction was arrested by collecting known volumes (~300 μl) of the effluent into 15 times the suspension volume of 0.5% isotonic glutaraldehyde.

Separation of single platelets and aggregates from red cells

Approximately 5 ml of effluent WB fixed in glutaraldehyde was carefully layered onto 40 ml of isotonic Percoll solution (density = 1.097 g ml^{-1}; Pharmacia, Dorval, Québec) in a 50-ml polycarbonate tube and centrifuged in a horizontal swingout rotor at $4000 \times g$ for 20 min. The hardened rbc

(density = 1.155 g ml^{-1}) formed a tight pellet at the bottom of the tube and hardened single platelets and aggregates (density = 1.04 g ml^{-1}) formed a thin layer at the glutaraldehyde-Percoll interface. The latter were carefully removed using a wide-tip polyethylene Pasteur pipette and resuspended in ~8.0 ml Percoll. The rbc did not entrap significant numbers of single platelets or aggregates as they migrated through the Percoll; at most 5% of platelets and 1% of aggregates co-sedimented with the rbc.

Particle concentration and size

The number, concentration, and volume of single platelets and aggregates were measured using an electronic particle and sizing system (Coulter Electronics) previously described (Bell et al., 1989a) to generate 250 class log-volume histograms over the volume range 1–10^5 μm^3. The number concentration per histogram class is $N(x_i)$, particle volume $v(x_i)$, and volume fraction $F(x_i) = N(x_i) \times v(x_i)$, where x_i is the mark of the ith class. Computer integration of the log-volume histograms yielded the number concentration and volume fraction of particles between lower and upper volume limits. Individual histograms from multiple donors were averaged, resulting in a histogram of the mean class volume fraction $\langle \Phi(x_i) \rangle$ normalized to the maximum class content at $\langle t \rangle = 0$ (Bell et al., 1989a).

As previously shown (Bell et al., 1990), there was no visible presence of cells or aggregates on the walls of the polyethylene tubing, and tests with aggregated suspensions demonstrated complete recovery of single platelets and aggregates after passage through the tubes.

Flow system for observing two-body collisions

The ghost cell or control serum suspensions flowed by gravity feed between 3-ml infusion and collecting reservoirs through vertically mounted 100-μm-diameter precision bore glass tubes. The latex spheres within the ghost cell suspensions were observed in the median, x,y-plane, normal to the optical axis (Fig. 1) through a Zeiss monocular microscope at 500× magnification. The tubes were mounted on glass slides attached to the platform of a hydraulically driven traveling microtube apparatus (Tha et al., 1986), and individual spheres were tracked in flow down the tube by matching the velocity of the upward-moving platform to that of the particles. Two-body collisions were photographed through the microscope using a 16-mm Locam II pin registration camera (Red Lake Laboratories, Santa Clara, CA) at film speeds from 100 to 300 frames/s.

Analysis of collisions

The cine films were analyzed by projecting them onto a Hewlett Packard 9118 Graphics Tablet. The angle of orientation, ϕ, of the projection of the axis of revolution of the collision doublets in the median plane (Fig. 1) was measured as a function of time during approach, apparent first contact ($\phi = -\phi_o$) and separation of the spheres ($\phi = +\phi_o'$), using an interactive computer program. Fig. 2 shows tracings from cine film of successive orientations of a collision doublet in the ghost cell suspension at 40–60-ms intervals. The measured lifetime of the doublets, τ_{meas}, obtained from the number of frames the spheres were in apparent contact (between the orientations marked with an asterisk in Fig. 2), was also recorded. The shear rate, $G(R)$, at the doublet center of rotation, a radial distance R from the tube axis (Fig. 1), was computed from an analysis of the particle velocity distribution, $u(R)$, obtained from the analysis of the trajectories of singlet spheres on cine films taken with the tube stationary. Over the experimental range of volume flow rates, $Q = 5 \times 10^{-3}$ to 3×10^{-2} μl s^{-1}, the ghost cell velocity distributions were blunted from the parabolic, with a region of plug flow in the center of the tube having a radius $R_c \leq 0.2\ R_o$ in which the spheres traveled with maximum and identical velocities, u_M. As previously found (Goldsmith and Marlow, 1979), the degree of blunting and R_c decreased with increasing flow rate. Fig. 3 illustrates such a blunted profile at $Q = 1.98 \times 10^{-2}$ μl s^{-1} (u_M = 1,510 μm s^{-1}), together with the distribution of shear rate, the latter obtained from the slopes of the best fit curve of the velocity distribution. The velocity profiles in the serum suspensions were parabolic, and the local shear rate, $G(R)$, was computed from the relation $G(R) = 2u_M R/R_o^2$.

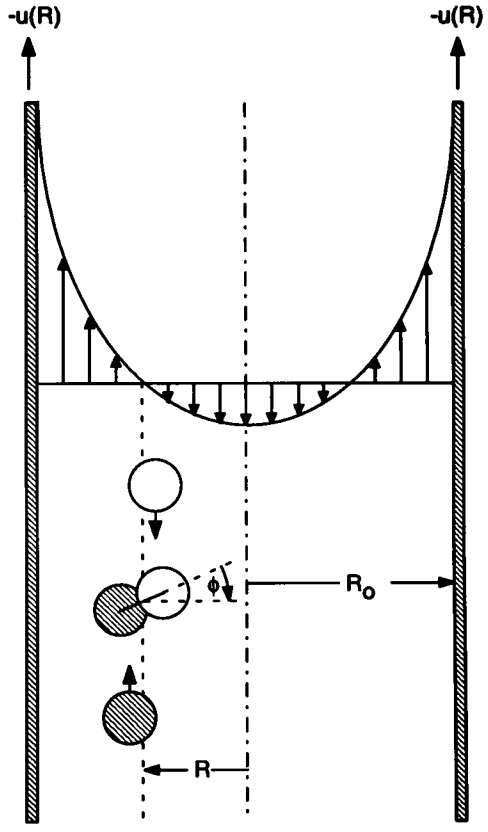

FIGURE 1 Schematic diagram of a collision of two equal-sized rigid spheres resulting in the transient formation of a doublet as viewed in the median plane of a circular tube of radius R_o. The clockwise rotation of the doublet, $d\phi/dt$, is followed by moving the tube upward with a velocity $u_3(R)$ equal but opposite to that of the downward flowing particle whose center is at a radial distance R from the tube axis. In the absence of other particles, the velocity distribution is parabolic as shown and the particle trajectories are undisturbed until their centers approach to within two diameter of each other. In the present experiments, however, the velocity distribution is blunted, as shown in Fig. 3, and the sphere paths are subject to marked radial excursions due to continuous collisions with the red cell ghosts.

The measured doublet lifetimes were compared with those in the control serum suspensions, as well as with those predicted by theory for collision doublets of rigid spheres in shear flow in the absence of electrostatic repulsive or van der Waals attractive interaction forces, Brownian motion, and interactions with other particles (Jeffery, 1922; Manley and Mason, 1952). Upon apparent contact at $\phi = -\phi_o$, the spheres rotate as a rigid dumbell, with variable angular velocity $d\phi/dt$, as would a spheroid of axis ratio r_e = 1.98 (Wakiya, 1971):

$$\frac{d\phi}{dt} = \frac{G}{r_e^2 + 1}\left(r_e^2 \cos^2\phi + \sin^2\phi\right), \tag{1}$$

which upon integration shows the rotation of the axis of revolution to be periodic:

$$\tan\phi = r_e \tan\left(\frac{Gt}{r_e + 1/r_e}\right) \tag{2a}$$

$$\cong r_e \tan\left(\frac{2Gt}{5}\right). \tag{2b}$$

The rotation is symmetrical about the plane of shear, until at an angle $\phi = +\phi_o'$, which is the reflection of the apparent collision angle, the particles

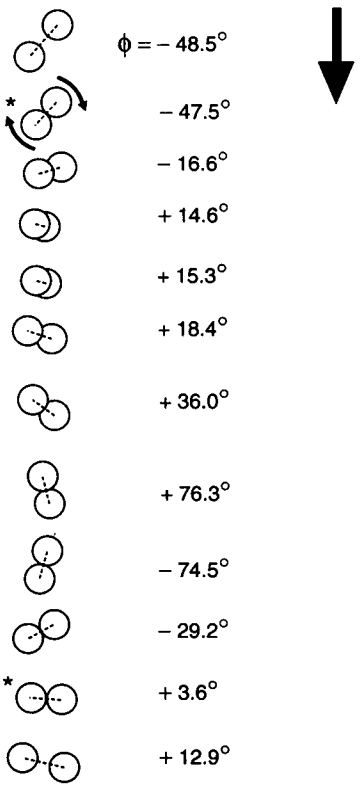

FIGURE 2 Tracings from the analysis of a cine film of the clockwise rotation of a doublet of latex spheres in a downward-flowing 40% ghost cell suspension at successive intervals from 40 to 60 ms from just before, to just after the spheres were in apparent contact (indicated by the asterisks). The centre of the doublet axis was at a radial distance 22.6 μm from the tube wall (at left; not shown), rotating in a clockwise direction. The local fluid shear rate, $G(R = 30.4\ \mu m) = 14.7\ s^{-1}$, at which the predicted doublet lifetime computed from Eq. 3 for $-\phi_o = 47.5°$, $\tau_{theor} = 0.17$ s. The measured lifetime, $\tau_{meas} = 0.50$ s: the particle rotated well past $\phi_o' = +47.5°$ until it reached $\phi_o = +3.6°$ of the next rotational orbit before separating.

separate. The predicted lifetime of the doublet is then, from Eq. 2b,

$$\tau_{theor} = \frac{5}{G} \tan^{-1}\left(\frac{1}{2} \tan \phi_o\right). \quad (3)$$

RESULTS

Effect of CP-CPK on platelet aggregation

Six female (26 ± 3 yr) and four male (48 ± 12 yr) donors were used in two series of 5 experiments, carried out at $\langle G \rangle = 41.9$ and 335 s^{-1}. In the first series, blood was infused with modified Tyrodes into the mixing chamber, and platelet aggregation was compared in the presence and absence of added CP-CPK. In each experiment, the effect of incubating the blood with enzyme for 30 min prior to flow was compared with that of adding the enzyme just before flow. In the second series of experiments, blood was infused with ADP at a final concentration of 0.2 μM. Here, the enzyme was added just before each run, and the results compared

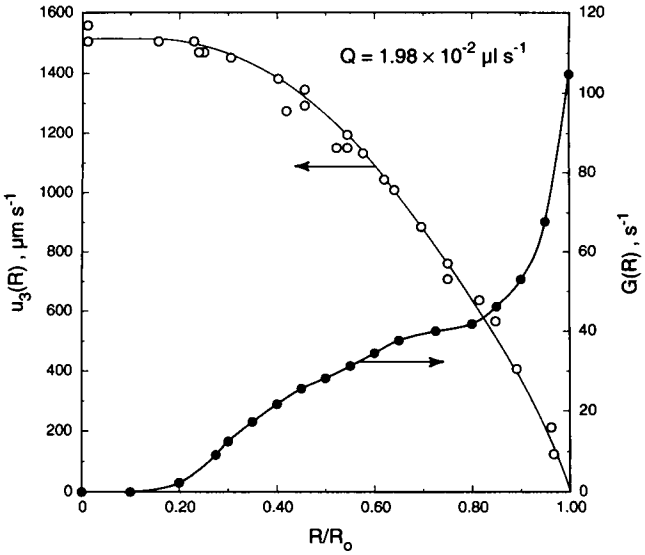

FIGURE 3 Velocity, $u_3(R)$ (○), and shear rate, $G(R)$ (●), as a function of dimensionless radial distance, R/R_o, in a 40% ghost red cell suspension undergoing flow at 1.98×10^{-2} μl s^{-1} in a 104-μm-diameter glass tube, as obtained from the measured velocities of tracer 2.54 μm latex spheres. The values of $G(R)$ were obtained from the slopes of the best-fit curve of the velocity distribution. The region of partial plug flow of maximum and uniform velocity (1510 μm s^{-1}) extends out to a radial distance $R_c = 0.13R_o$.

with control runs in the absence of added CP-CPK in which modified Tyrodes, instead of ADP, was infused. The mean hematocrits of the blood prior to flow were 38.2 ± 1.9% (SD) and 39.5 ± 3.8%, in the first and second series, respectively.

Aggregation in the absence of added ADP

Single platelet concentration. As previously observed (Bell et al., 1990), in the absence of added agonist, there was significant platelet aggregation in whole blood at both shear rates. The extent of aggregation was more marked at $\langle G \rangle = 41.9\ s^{-1}$, where there was a decrease of 42.4 ± 6.9% (SEM) in single cells at $\langle t \rangle = 43$ s (Fig. 4 *a* and Table 1), compared to a decrease of 12.7 ± 2.9% at $\langle G \rangle = 335\ s^{-1}$ (Fig. 4 *b*). The figures show that CP-CPK, whether added at the time of the run, or 30 min before the run, completely abolished aggregation; the percentage of single cells remaining at $\langle t \rangle = 43$ s actually increased to 104.6 ± 6.8% and 114.5 ± 5.4% for 0 and 30 min incubation, respectively, at the lower shear rate. The corresponding values at the higher shear rate were 103.4 ± 4.2% and 99.4 ± 6.1%. The observed initial increase in the number of single platelets at both shear rates in the presence of enzyme is significant, and reflects the break-up of small aggregates of <8 cells, which could be seen in diluted samples of the suspensions under the microscope.

Aggregate size. The patterns of single platelet and aggregate size distribution at $\langle G \rangle = 41.9$ and 335 s^{-1} after flow at $\langle t \rangle = 43$ s, in the presence and absence of CP-CPK, are

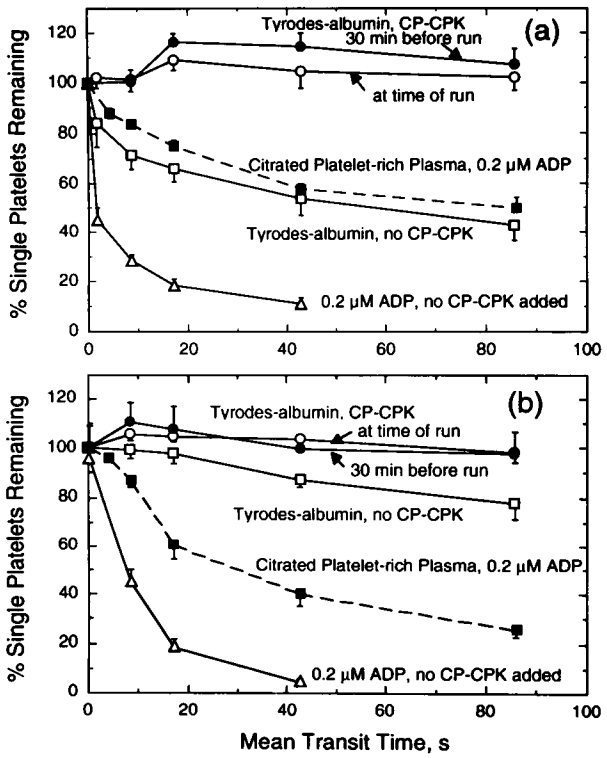

FIGURE 4 Effect of adding CP-CPK on the time course of platelet aggregation in whole blood as measured by the disappearance of single cells. (*a*) $\langle G \rangle = 41.9\ s^{-1}$; (*b*) $\langle G \rangle = 335\ s^{-1}$. Aggregation in the absence of added agonist, although much less than in the presence of 0.2 μM ADP, is abolished by adding CP-CPK. For comparison, aggregation in cPRP at 0.2 μM ADP previously measured (Bell et al., 1989b) is also shown.

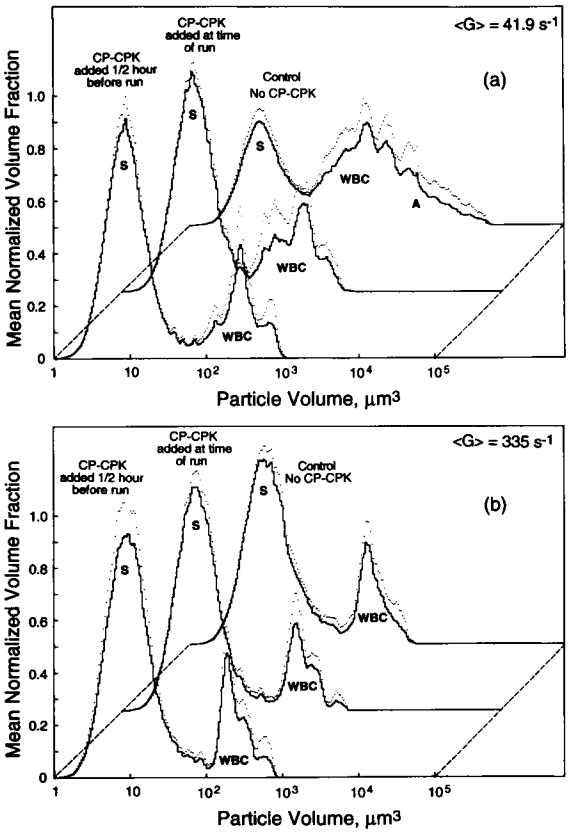

FIGURE 5 Effect of adding CP-CPK on the formation of platelet aggregates in whole blood, (*a*) at $\langle G \rangle = 41.9\ s^{-1}$, (*b*) at $\langle G \rangle = 335\ s^{-1}$ after flow for a mean transit time of 43 s. Three-dimensional diagram of plots of the mean normalized volume fraction against particle volume. The two peaks correspond to singlets (S) and white cells (WBC). Aggregate formation (A) in the absence of added CP-CPK is considerably greater at $\langle G \rangle = 41.9\ s^{-1}$ than at $\langle G \rangle = 335\ s^{-1}$.

shown in Fig. 5. Here, the mean normalized volume fraction for each set of five experiments has been plotted against particle volume over the range from 1 to 10^5 μm^3 in a three-dimensional diagram. The suspensions containing CP-CPK each exhibit two peaks, the first of which corresponds to single platelets (S) with a modal volume of ~8 μm^3. These peaks followed a log-normal distribution (mean cell volume from 5.95 to 6.61 μm^3) with relatively few aggregates present. The second, smaller peaks, having a modal volume of ~250 μm^3, correspond to white blood cells (WBC). By contrast, in the control set of experiments with no added enzyme, the heights of the singlet peak decreased significantly and the distributions were skewed toward higher particle volume. At $\langle G \rangle = 41.9\ s^{-1}$ (Fig. 5 *a*), a significant number of aggregates (A), between 10^3 and 10^4 μm^3 volume, were present in the controls. At $\langle G \rangle = 335\ s^{-1}$ (Fig. 5 *b*), the aggregates were <200 μm^3 in volume, confined to the upslope of the WBC peak.

TABLE 1 Comparison of spontaneous and ADP-induced platelet aggregation

Shear rate s^{-1}	Mean transit time s	% Platelets aggregated ± SEM		
		Tyrodes-albumin; WB	0.2 μM ADP; WB	0.2 μM ADP; c-PRP
41.9	8.6	28.3 ± 5.8	71.5 ± 2.3	16.4 ± 1.9
	43	42.4 ± 6.9	88.9 ± 6.9	42.4 ± 2.3
335	8.6	1.0 ± 3.4	55.2 ± 5.3	13.1 ± 2.9
	43	12.7 ± 2.9	95.5 ± 1.2	60.0 ± 4.6

Aggregation in the presence of added ADP

Single platelet concentration. Fig. 6, *a* and *b*, illustrates the rate and extent of aggregation at $\langle G \rangle = 41.9$ and $335\ s^{-1}$, with and without added CP-CPK at the time of the run, compared to runs with no added CP-CPK with and without agonist. It can be seen that, after an initial decrease in single platelet concentration at a rate considerably smaller than in the absence of CP-CPK, the enzyme halted the aggregation. At both values of $\langle G \rangle$, the mean maximum decrease in single platelets was 30%, and occurred at $\langle t \rangle = 17$ s. It was followed by a slight but not statistically significant increase of 2.5% and 8.3% in the mean single platelet concentration at $\langle G \rangle = 41.9$ and $335\ s^{-1}$, respectively. It is evident that the extent of aggregation in the absence of CP-CPK was much greater at 0.2 μM ADP (at $\langle t \rangle = 43$ s, only 11.1 ± 2.4% and 4.5 ± 1.2% single cells remained at $\langle G \rangle = 41.9$ and 335

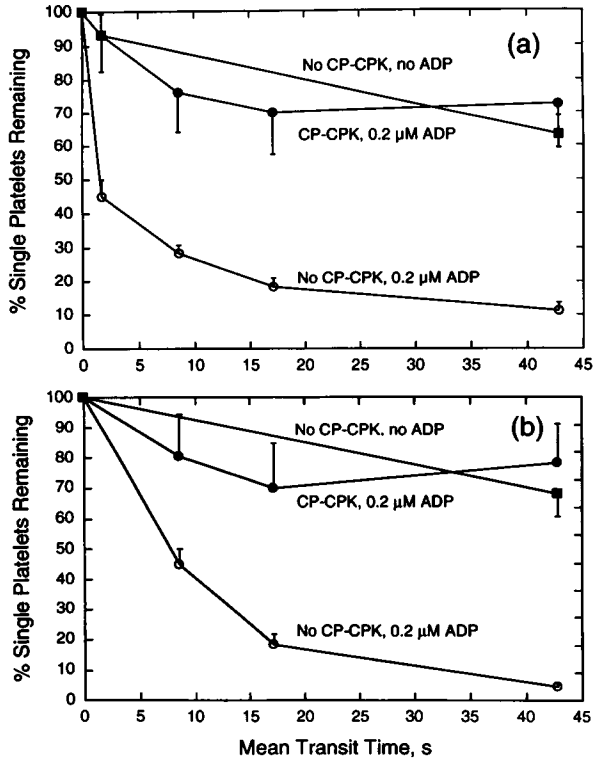

FIGURE 6 Effect of ADP on the time course of platelet aggregation with and without adding CP-CPK. Plot as in Fig. 4, (*a*) at $\langle G \rangle = 41.9\ s^{-1}$, (*b*) at $\langle G \rangle = 335\ s^{-1}$. With 0.2 μM ADP, the enzyme initially reduces the rate and extent of aggregation, then arrests and reverses the aggregation.

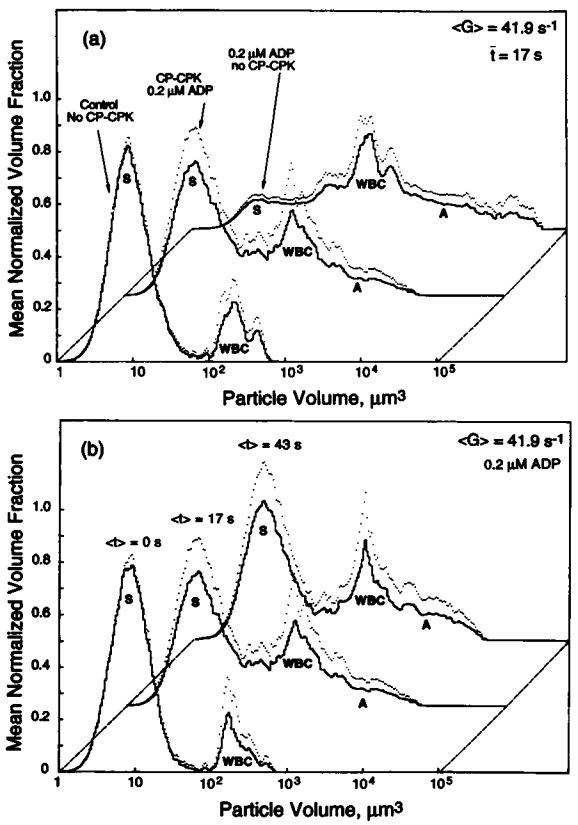

FIGURE 7 Plot as in Fig. 5 of the effect of CP-CPK on patterns of aggregate formation in the presence of 0.2 μM ADP; $\langle G \rangle = 41.9\ s^{-1}$. (*a*) After flow for a mean transit time of 17 s showing the much lower singlet peak (S) and the broader aggregate distribution (A) in the absence of CP-CPK. (*b*) After flow for a mean transit time of 43 s showing the time course of aggregate formation with 0.2 μM ADP. The singlet peak is higher and the aggregate size distribution narrower at $\langle t \rangle = 43$ s, as the extent of aggregation is reversed.

s^{-1}, respectively) than in the control runs in which modified Tyrodes was infused (63.2 ± 5.7% and 68.0 ± 7.4% single cells, respectively).

Aggregate size. The effect of CP-CPK on the patterns of single platelet and aggregate size distribution with 0.2 μM ADP at $\langle G \rangle = 41.9\ s^{-1}$ after flow for $\langle t \rangle = 17$ s, the maximum extent of aggregation in the presence of CP-CPK, are shown in Fig. 7 *a*. The considerably larger aggregation in the absence of added CP-CPK is clearly evident from the much greater reduction in the height of the singlet peak from that of the control at $\langle t \rangle = 0$ s, as well as by the much greater number of aggregates of volume $>10^4\ \mu m^3$. The pattern of aggregate growth in the presence of CP-CPK at $\langle G \rangle = 41.9\ s^{-1}$ is shown in Fig. 7 *b*. It can be seen that, when compared to the distribution of aggregate size at $\langle t \rangle = 17$ s, the distribution at $\langle t \rangle = 43$ s was shifted toward smaller values.

Collisions between latex microspheres in ghost cell and serum suspensions

Five series of experiments were carried out, each with separate preparations of ghost cell and PEO-coated latex sphere suspensions. Two control experiments were carried in separate preparations of PEO-coated latex spheres in serum. The number of collisions observed and analyzed in each cine film varied from 25 to 85. In the ghost cells, a total of 320 collisions were analyzed at shear rates, $G(R)$, computed at the doublet center of rotation, from 5 to 90 s^{-1}. In serum, a total of 90 collisions were analyzed at $G(R)$ from 10 to 35 s^{-1}.

Distribution of ratio τ_{meas}/τ_{theor}

Table 2 gives the mean values and standard deviations of τ_{meas}/τ_{theor} in each of the seven experiments, and Fig. 8 compares histograms of the differential number distribution of doublets in serum and ghost cell suspensions as a function of increasing τ_{meas}/τ_{theor}. The table also gives the mean values of $G(R)$, which were appreciably lower in the first two ghost cell experiments. It is evident that, whereas there is a wide scatter in τ_{meas}/τ_{theor} in the ghost cell suspensions with more than half the doublets having lifetimes longer than predicted, and an overall mean value of 1.614 ± 1.795 (SD), in serum there is a much smaller scatter with a mean value of 1.001 ± 0.312 (SD), as predicted for two-body collisions between rigid spheres. Of a total of 320 doublets

TABLE 2 Ratio of measured to theoretical doublet lifetimes

Experiment No.	n*	Fraction with τ_{meas}/τ_{theor} <1.0	Fraction with τ_{meas}/τ_{theor} ≥1.0	$\langle\tau_{meas}/\tau_{theor}\rangle$ ± SD	$\langle G\rangle$, s^{-1} ± SD
Ghost cell suspensions					
1	91	0.407	0.593	2.179 ± 2.879	19.23 ± 9.20
2	85	0.259	0.741	1.780 ± 1.168	20.22 ± 10.27
3	52	0.500	0.500	1.306 ± 1.053	39.99 ± 25.22
4	68	0.691	0.309	0.967 ± 0.666	38.31 ± 14.10
5	24	0.292	0.708	1.378 ± 0.808	34.56 ± 11.84
Mean value		0.434	0.566	1.614 ± 1.795	27.91 ± 17.16
Serum					
6	40	0.425	0.575	1.071 ± 0.335	25.34 ± 6.10
7	50	0.620	0.380	0.944 ± 0.287	26.13 ± 6.73
Mean value		0.522	0.478	1.001 ± 0.317	25.74 ± 6.41

*Number of collision doublets.

analyzed in the ghost cell suspensions, 43.4% had lifetimes shorter than predicted from Eq. 2, and 75% of these had $\tau_{meas}/\tau_{theor} > 0.5$. Of the 181 particles with lifetimes greater than those predicted, the majority (73%) were in the range $1.0 < \tau_{meas}/\tau_{theor} < 2.5$; 20% were in the range $2.5 < \tau_{meas}/\tau_{theor} < 5.0$; the remaining 7% had values of τ_{meas}/τ_{theor} as high as 20. By contrast, in serum, the doublet lifetimes were more equally distributed about the theoretical value 1.0 (43 doublets with lifetimes less than and 47 with lifetimes greater than theoretical), and 70% of collisions were in the range $0.70 < \tau_{meas}/\tau_{theor} < 1.30$, the minimum and maximum values of τ_{meas}/τ_{theor} being 0.41 and 1.91, respectively.

Table 3 gives the distributions and mean values of τ_{meas}/τ_{theor} according to shear rate, arranged in ascending ranges of 10 and 20 s^{-1}. It is evident that, in the ghost cell suspensions, there was no statistically significant correlation of the mean τ_{meas}/τ_{theor} with shear rate range, although the fraction of doublets with lifetimes less than those predicted was significantly higher at $1 < G < 20$ s^{-1} (54%) than at $21 < G < 90$ s^{-1} (37%). In the serum suspensions also, the fraction of doublets with lifetimes less than predicted decreased with increasing shear rate (Table 3).

A correlation of τ_{meas}/τ_{theor} with apparent angle of contact, $-\phi_o$, was also tested in the ghost cell suspensions, and there was a statistically significant decrease in the fraction of doublets with lifetimes longer than predicted, with in-

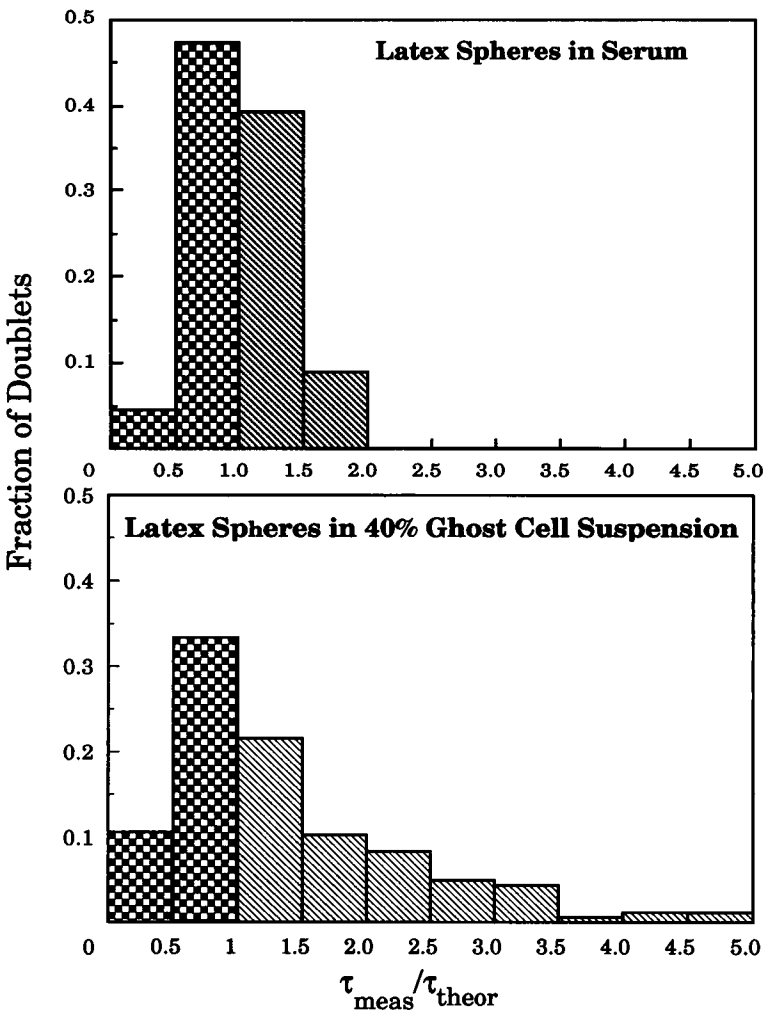

FIGURE 8 Two-body collisions of 2.5 μm latex microspheres in 40% ghost cell suspensions, compared to that in serum flowing through 104-μm-diameter tubes. Histogram of the differential number distribution of doublets as a function of the ratio of measured to theoretical doublet lifetimes, computed from Eq. 3. The mean $\tau_{meas}/\tau_{theor} = 1.61$ for the ghost cell suspensions, compared to 1.01 for the serum suspensions.

TABLE 3 Ratio of measured to theoretical doublet lifetimes as a function of shear rate

G s^{-1}	n*	Fraction having τ_{meas}/τ_{theor} <1.0	Fraction having τ_{meas}/τ_{theor} ≥1.0	$\langle\tau_{meas}/\tau_{theor}\rangle$ ± S.D.
Ghost cell suspensions				
1–10	33	0.636	0.364	1.178 ± 1.298
11–20	87	0.505	0.495	1.511 ± 1.402
21–30	86	0.314	0.686	1.694 ± 2.159
31–40	56	0.464	0.536	1.761 ± 2.334
41–50	27	0.370	0.630	1.621 ± 1.320
51–70	23	0.391	0.609	1.563 ± 0.960
71–90	8	0.250	0.750	2.056 ± 1.151
Total	320	Mean	value	1.614 ± 1.795
Serum				
11–20	17	0.765	0.235	0.846 ± 0.359
21–30	48	0.583	0.417	0.993 ± 0.310
31–40	25	0.315	0.685	1.120 ± 0.245
Total	90	Mean	value	1.001 ± 0.317

*Number of collision doublets.

creasing $|\phi_o|$; thus the fraction having $\tau_{meas}/\tau_{theor} > 1.0$ was 87%, 55%, and 47%, respectively, in the ranges $-\phi_o$ = 1–30°, 31–60°, and 61–90°. The corresponding values for $\tau_{meas}/\tau_{theor} > 2.0$ were 51%, 23%, and 9%, respectively. Moreover, as shown in Table 4, there were significant differences in the mean τ_{meas}/τ_{theor} between each of the three ranges.

Furthermore, statistical analysis showed that, as indicated in Table 5, in each of the ranges $-\phi_o$ = 31–45°, 46–60°, and 61–75°, in which there were sufficient numbers of collisions in serum, the values of τ_{meas}/τ_{theor} for doublets with lifetimes greater than predicted were significantly lower in serum than in the ghost cell suspensions. The table also shows that there was no significant correlation between τ_{meas}/τ_{theor} and angle of collision.

Doublet rotations

As previously found with the translational motions of single latex spheres in ghost cell suspensions (Goldsmith, 1971), the angular motions of collision doublets were subject to erratic fluctuations. Fig. 9 shows plots of the time course of the ϕ-orientation of the axes of two doublets just before, during, and after a collision, and compares the angular motion *during the collision* with that computed from theory (Eq. 2) for undisturbed freely rotating doublets between the orientations $\phi = -\phi_o$ and $\phi = +\phi_o$ at the same local shear rate. In the upper panel (Fig. 9 *a*), at G = 4.6 s^{-1}, the doublet had a lifetime greater than that predicted (τ_{meas} = 0.21 s, τ_{theor} = 0.16 s). In the lower panel (Fig. 9 *b*), at G = 22.5 s^{-1}, the lifetime was shorter than predicted (τ_{meas} = 0.18 s, τ_{theor} = 0.26 s). It is evident that, in both cases, there were times at which there was reversal of the direction of rotation, and fluctuations of the angular velocity of the doublet axis, during the period of apparent contact of the spheres (between the vertical dashed lines in the figures). However, for the doublet in the upper panel there was a period > $0.3\tau_{theor}$ during which rotation was inhibited, there being virtually no increase in ϕ. This was not the case for the doublet in the lower panel. To test whether this difference characterized many particles having $\tau_{meas}/\tau_{theor} > 1$, the time course of rotation of 67 doublets having $\tau_{meas}/\tau_{theor} > 2.0$ was compared with 107 doublets having $\tau_{meas}/\tau_{theor} < 1.0$. The characteristics studied were 1) reversal of rotation of not less than 5°, and 2) a period of > $0.2\tau_{theor}$ during which time ϕ fluctuated, rather than exhibiting a continuous increase (Fig. 9 *a*). The analysis showed that 57% of doublets having $\tau_{meas}/\tau_{theor} > 2.0$ exhibited both fluctuations and major reversals in ϕ; an additional 10% showed major reversals in ϕ only, and 13% fluctuations in ϕ only. In contrast, only 20% of doublets having $\tau_{meas}/\tau_{theor} < 1.0$ exhibited both fluctuations and major reversals in ϕ, whereas an additional 21% showed major reversals in ϕ only, and 21% fluctuations in ϕ only. It was also noted that, as shown in Figs. 2 and 9 *a*, a characteristic of many doublets with lifetimes greater than predicted was their rotation past the orientation $+\phi_o' = -\phi_o$ before separating.

DISCUSSION

Spontaneous aggregation of platelets in whole blood

The spontaneous aggregation of platelets and its complete inhibition by the CP-CPK enzyme system observed at both mean tube shear rates support the hypothesis that sublytic

TABLE 4 Ratio of measured to theoretical doublet lifetimes in ghost cells as a function of angle of collision, $-\phi_o$

$-\phi_o$* degrees	n‡	Fraction having τ_{meas}/τ_{theor} ≥1.0	Fraction having τ_{meas}/τ_{theor} ≥2.0	$\langle\tau_{meas}/\tau_{theor}\rangle$ ± SD Averaged over 15°		Averaged over 30°	
1–15	17	1.000	0.706	3.743 ± 3.590			
16–30	49	0.755	0.429	2.630 ± 3.084§	$P < 0.005$	2.917 ± 3.234	
31–45	58	0.517	0.190	1.352 ± 1.043			$P < 0.001$
46–60	96	0.531	0.240	1.394 ± 0.989§		1.378 ± 1.006	
61–75	66	0.515	0.121	1.201 ± 0.727	$P < 0.05$		$P < 0.01$
76–90	34	0.353	0.059	0.950 ± 0.603		1.116 ± 0.695	

*Angle of collision when spheres are first seen to make apparent contact.
‡Number of collision doublets.
§Not significantly different from previous value.

TABLE 5 Ratio of measured to theoretical doublet lifetimes: serum compared to ghost cell suspensions

$-\phi_o$ degrees	$\langle\tau_{meas}/\tau_{theor}\rangle \pm$ SD				Significance	
	Suspensions in serum		Ghost cell suspensions		Ghosts vs serum	
	<1*	≥1‡	<1*	≥1‡	<1*	≥1‡
31–45	0.714 ± 0.141 (n = 11)	1.161 ± 0.100 (n = 12)	0.662 ± 0.189 (n = 28)	1.996 ± 1.103 (n = 30)	n.s.§	$P < 0.001$
46–60	0.772 ± 0.155 (n = 25)	1.273 ± 0.203 (n = 17)	0.645 ± 0.180 (n = 45)	2.055 ± 0.938 (n = 51)	$P < 0.005$	$P < 0.001$
61–75	0.766 ± 0.155 (n = 9)	1.105 ± 0.074 (n = 6)	0.652 ± 0.209 (n = 32)	1.718 ± 0.658 (n = 34)	n.s.§	$P < 0.001$

*Computed from τ_{meas}/τ_{theor} values < 1.
‡Computed from τ_{meas}/τ_{theor} values ≥ 1.
§Not significantly different.

ADP leakage is responsible for the effect. It has been argued that the formation of aggregates in WB is due to a combination of platelet activation during blood extraction and handling (as evidenced by some shape change in ~30% of the cells, a prerequisite for aggregation; Frojmovic and Milton, 1982; Milton and Frojmovic, 1984) and the higher collision frequencies in WB over those in PRP (see below). Such weakly bound aggregates would be stable only at the lower shear rate. However, activation of platelets is also observed in PRP, yet no spontaneous shear-induced platelet aggregation or release is detected in the preparation of c-PRP (Bell et al., 1989b; Goldsmith et al., 1994). It is much more likely that nucleotide leakage comes from intact red blood cells, a view supported by previous experiments in which we showed that neither TXA_2-dependent release of platelet granule ADP nor red cell lysis occurred in spontaneous or ADP-induced platelet aggregation (Bell et al., 1990). Moreover, spontaneous aggregation in the previous, as well as in the present, experiments was much greater at the lower shear rate (Fig. 4), making it unlikely that shear-induced platelet activation contributed significantly to ADP release and platelet aggregation. The maximum (wall) shear stresses prevailing in the tube flow experiments, 0.14 and 1.13 N m^{-2} at $\langle G\rangle$ = 41.9 and 335 s^{-1}, respectively, are far below the observed threshold for spontaneous platelet aggregation and release at room temperature in PRP (Belval and Hellums, 1986; Brown et al., 1975; Ikeda et al., 1991) and in WB (Jen and McIntire, 1984; Dewitz et al., 1978).

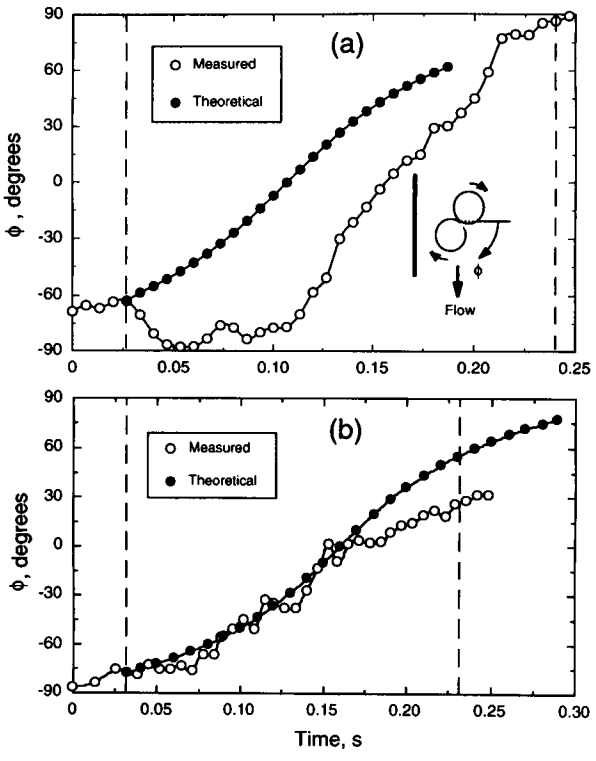

FIGURE 9 Erratic time course of the ϕ-orientation of the axis of collision doublets (○) compared to that predicted by theory for freely rotating doublets formed at the same initial $\phi = -\phi_o$ and local shear rate (●), which would separate at the mirror image position, $\phi = +\phi_o'$, Eq. 2. (*a*): $\tau_{meas} > \tau_{theor}$; $G(R)$ = 4.6 s^{-1}; (*b*): $\tau_{meas} < \tau_{theor}$, $G(R)$ = 22.5 s^{-1}. The period of apparent contact between the spheres is given by the interval between the vertical dashed lines. Note the period between t = 0.05 and 0.10 s when the rotation of the doublet in (*a*) is impeded.

How important is spontaneous compared to ADP-induced aggregation? The results shown in Table 1 indicate that the mean initial rates of spontaneous aggregation over the first 8.6 s of flow, as measured by the percentage decrease in single platelets, are only significant at the lower shear rate, being 40% and 2% of those in ADP-induced aggregation at G = 41.9 and 335 s^{-1}, respectively. Similarly, the mean extents of spontaneous aggregation at $\langle t\rangle$ = 43 s are 48% and 13% of those in 0.2 μM ADP-induced aggregation at $\langle G\rangle$ = 41.9 and 335 s^{-1}, respectively. As shown in Fig. 4 and Table 1, the rates and extent of spontaneous aggregation in WB at the lower shear rate are close to those observed in cPRP with 0.2 μM ADP, whereas at $\langle G\rangle$ = 335 s^{-1} they are markedly lower. Both wall and mean shear rates in the large vessels of the circulation are estimated to be in excess of 250 s^{-1} (Goldsmith and Turitto, 1986). Shear stresses of >8 Nm^{-2} (shear rates > 2,300 s^{-1}), at which spontaneous platelet activation is significant, may occur at the wall of arterioles in the microcirculation and at peak systole during exercise in the major arteries when aggregates formed are quickly convected away. Spontaneous platelet aggregation is therefore expected to be of little consequence in the circulation of healthy individuals.

Shear-induced platelet collisions in whole blood

Physical effect of red cells on collision frequency

Red blood cells markedly increase the diffusivity of platelets (and platelet-sized microspheres) in plasma flowing through small tubes, the effective translational diffusion coefficient increasing by at least two orders of magnitude (Turitto et al., 1972; Goldsmith, 1971; Goldsmith and Marlow, 1979). In addition, migration of rbc away from the vessel wall is believed to be responsible for producing a near-wall excess of platelets (Tangelder et al., 1985) and platelet-sized microspheres (Eckstein et al., 1988; Eckstein and Belgacem, 1991). An increased diffusivity, aided by an enhanced peripheral platelet concentration, would be expected to lead to an increased cell wall collision rate, and this can explain the much greater number density of platelets adhering to the wall of blood vessels in WB than in PRP (Turitto and Baumgartner, 1975; Feuerstein et al., 1975; Karino and Goldsmith, 1979; Aarts et al., 1983). By contrast, the increased platelet diffusivity is expected to have a much smaller effect on the rate of platelet-platelet collisions and hence the formation of free-flowing aggregates. The argument is based on the fact that, except at the lowest shear rates, the shear-induced two-body collision frequency is much greater than the effective Brownian motion-induced two-body collision frequency. In terms of classical two-body collision theory (Smoluchowski, 1917; Goldsmith and Mason, 1967) the collision frequency, J_s, between platelets treated as rigid spheres would be given by

$$J_s = \frac{32}{3} G b^3 N \tag{4}$$

where N is the number concentration of spheres of radius b. The Brownian motion two-body collision frequency, J_D, is given by (Smoluchowski, 1917)

$$J_D = 16\pi b N D_r \tag{5}$$

where D_r is now the effective diffusion coefficient, based on the radial dispersion of the particles in tube flow (Goldsmith, 1971). Calculations based on measured radial dispersion coefficients of 2×10^{-11} $m^2 s^{-1}$ in ghost cell-latex sphere suspensions (Goldsmith and Marlow, 1979) indicate that the two-body collision frequency in WB would increase by 156% at $\langle G \rangle = 41.9$ s^{-1}, but only by 19% at $\langle G \rangle = 335$ s^{-1} over that in PRP (Bell et al., 1990). These values could not explain increases of 7 to 15 times in initial collision frequencies as computed from the decrease in initial single platelet number concentration (Bell et al., 1990).

Physical effect of red cells on collision efficiency

The present work with the ghost cell-latex sphere model suspensions sought to provide an alternate explanation in terms of an increased collision efficiency, i.e., an increase in the fraction of collisions resulting in permanent aggregate formation. The collision capture efficiency $\alpha_o = J_s/J_c$, where J_c is the two-body capture frequency. We tested the hypothesis that an increased α_o may result from an increased time of interaction of cells during collision, i.e., an increased doublet lifetime. The results have shown that, at concentrations of latex spheres in 40% ghost cell suspensions comparable to those of platelets in whole blood, the mean lifetimes of colliding doublets increased by about 60% over that predicted to occur in the absence of ghost cells. Such an increase was not seen in the control experiments in serum in which the mean lifetime was that predicted by theory for collision doublets of rigid spheres with a much narrower distribution about the mean value (Fig. 8). Over 55% of observed collisions in the ghost cell suspensions had lifetimes greater than predicted, and of these, 20% had lifetimes from 2.5 to 5 times greater than predicted (Table 2). None of the doublets in serum had lifetimes greater than 1.9 times those predicted. In the case of activated platelets, such increased doublet lifetimes would increase the probability of forming a fibrinogen cross-bridge between the GPIIb-IIIa receptors on adjacent interacting cells, the likely mechanism of ADP-induced platelet aggregation (Frojmovic et al., 1991; Sung et al., 1993). The time available for stable bond formation during collision is an important factor because the cells express time-dependent changes in the degree of activation. In the in vivo situation, the doublet lifetimes are expected to be very short: wall shear rates are estimated to increase from ~300 to 1,100 s^{-1} in going from major to the smallest arteries (Goldsmith and Turitto, 1986). The corresponding mean lifetimes of a doublet (averaged over all possible collision orientation angles), given by $\langle \tau \rangle = 5\pi/6G$ (Goldsmith and Mason, 1967), would decrease from 8.7 to 2.3 ms.

From the analysis of the rotations of the doublets, it appears that impedance of doublet rotation is the likely mechanism by which the doublet lifetime is extended beyond the period predicted by theory for single isolated particles. The jostling of the cells in shear flow as they continually collide with each other, clearly visible on the cine films, appears to prevent some doublets from rotating, and indeed leads to momentary reversal of the direction of rotation. Yet, one would have expected that, given enough time, the periods of impeded rotation would, on average, be offset by periods of accelerated rotation. Indeed, this is the case for the doublet shown in Fig. 9 *a* where the angular velocity between $t = 0.10$ and 0.20 s is significantly faster than predicted by theory, yet separation was delayed until ϕ reached almost 90° (doublet axis aligned with the flow). It is possible that the reason for the statistically significant decrease of τ_{meas}/τ_{theor} with increasing angle of collision $-\phi_o$ (Table 4) is due to the fact that at low collision angle the doublet lifetime is too short to allow a sufficient period of accelerated rotation to follow a period of impeded rotation.

It remains then to comment on the observed scatter in the ratio of measured to theoretical doublet lifetimes seen in the suspensions of latex in serum. Because the spheres are of colloidal size, and suspended in serum having a low viscos-

ity η (1.6 mPa s at 23°C), the scatter could be due to Brownian motion. Van de Ven et al. (1980) have shown that the spread σ in the distribution of the dimensionless period of rotation, TG, increases with increasing rotary Brenner number, Br_r:

$$\sigma/TG = k\, Br_r^{-1/2} \quad (6)$$

where $Br_r = G/2D_r$, D_r being the rotary diffusion coefficient, defined as:

$$D_r = \frac{kT_K}{K\pi\eta b^3} \quad (7)$$

where k is the Boltzmann constant, T_K the absolute temperature, K the rotary resistance coefficient normal to the line of centers (= 29.92 for a doublet of touching spheres), and b is the sphere radius. In serum, $D_r = 0.014$ at 23 °C, and Br_r increases from 350 to 1000 as G increases from 10 to 30 s^{-1}. Theory, supported by experiment (van de Ven et al., 1981; Takamura et al., 1981) shows that, depending on the orientation of the doublet axis with respect to the vorticity axis, σ/TG would vary from 5 to 8% at the lower Br_r, and from 3 to 5% at the higher Br_r, a spread lower than the 31% (S.D.) observed in the ratio τ_{meas}/τ_{theor}. The difference is likely due to experimental error in the measurement of doublet lifetime, accurate to within one or two frames of the cine film. Thus, doublets with short lifetimes (5–10 frames) may be subject to errors from 20 to 40%. In fact, of the 14 doublets in serum having $\tau_{meas}/\tau_{theor} < 0.7$ and the 12 doublets having $\tau_{meas}/\tau_{theor} > 1.3$, 20 had lifetimes of <10 frames of the cine film. By contrast, a similar analysis of the doublets in ghost cell suspensions showed that of the 74 particles with $\tau_{meas}/\tau_{theor} < 0.7$ and 140 particles with $\tau_{meas}/\tau_{theor} > 1.3$, only 57 had lifetimes of <10 frames. Again, there is a striking difference between doublet behavior in serum and in ghost cell suspensions.

REFERENCES

Aarts, P. A. M. M., P. A. Bolhuis, K. S. Sakariassen, R. M. Heethar, and J. J. Sixma. 1983. Red blood cell size is important for adhesion of platelets to artery endothelium. *Blood.* 62:214–217.

Armstrong, R., J. A. May, W. Lösche, and S. Heptinstall. 1995. Factors that contribute to spontaneous platelet aggregation and streptokinase-induced aggregation in whole blood. *Thromb. Haemost.* 73:297–303.

Bell, D. N., S. Spain, and H. L. Goldsmith. 1989a. The ADP-induced aggregation of human platelets in flow through tubes. I. Measurement of the concentration and size of single platelets and aggregates. *Biophys. J.* 56:817–828.

Bell, D. N., S. Spain, and H. L. Goldsmith. 1989b. The ADP-induced aggregation of human platelets in flow through tubes. II. Effect of shear rate, donor sex, and ADP concentration. *Biophys. J.* 56:829–843.

Bell, D. N., S. Spain, and H. L. Goldsmith. 1990. The effect of red blood cells on the ADP-induced aggregation of human platelets in flow through tubes. *Thromb. Haemost.* 63:112–121.

Belval, T., and J. D. Hellums. 1984. The analysis of shear-induced platelet aggregation with population balance mathematics. *Biophys. J.* 50: 479–487.

Brown, C. H., L. B. Leverett, C. W. Lewis, C. P. Alfrey, and J. D. Hellums. 1975. Morphological, biochemical and functional changes in human blood platelets subjected to shear stress. *J. Lab. Clin. Med.* 86:462–471.

Dewitz, T. S., R. R. Martin, R. T. Solis, J. D. Hellums, and L. V. McIntire. 1978. Microaggregate formation in whole blood exposed to shear stress. *Microvasc. Res.* 16:263–271.

Eckstein, E. C., and F. Belgacem. 1991. Model of platelet transport in flowing blood with drift and diffusion terms. *Biophys. J.* 60:53–69.

Eckstein, E. C., A. W. Tilles, and F. J. Millero. 1988. Conditions for the occurence of large near-wall excesses of small particles during blood flow. *Microvasc. Res.* 36:31–39.

Feuerstein, I. A., J. M. Brophy, and J. L. Brash. 1975. Platelet transport and adhesion to reconstituted collagen and artificial surfaces. *Trans. Am. Soc. Artif. Intern. Organs* 21:427–434.

Fox, S., M. E. Burgess-Wilson, S. Heptinstall, and J. R. Mitchell. 1982. Platelet aggregation in whole blood determined using the Ultra-Flo 100 platelet counter. *Thromb. Haemost.* 48:327–329.

Frojmovic, M. M., and J. G. Milton. 1982. Human platelet size, shape and related functions in health and disease. *Physiol. Rev.* 62:185–261.

Frojmovic, M. M., T. E. O'Toole, E. F. Plow, J. C. Loftus, and M. Ginsberg. 1991. Platelet glycoprotein II_b-III_a ($\alpha_{IIb}\beta_3$ integrin) confers fibrinogen- and activation-dependent aggregation on heterologous cells. *Blood.* 78:369–376.

Goldsmith, H. L. 1971. Red cell motions and wall interactions in tube flow. *Fed. Proc.* 30:1578–1588.

Goldsmith, H. L., and J. C. Marlow. 1979. Flow behavior of erythrocytes. II. Particle motions in sheared suspensions of ghost cells. *J. Colloid Interface Sci.* 71:383–407.

Goldsmith, H. L., and S. G. Mason. 1967. The microrheology of dispersions. *In* Rheology: Theory and Applications, Vol. 4. F. R. Eirich, editor. Academic Press, New York. 85–250.

Goldsmith, H. L., M. M. Frojmovic, S. Braovac, F. McIntosh, and T. Wong. 1994. Adenosine diphosphate-induced aggregation of human platelets in flow through tubes. III. Shear and extrinsic fibrinogen-dependent effects. *Thromb. Haemost.* 71:78–90.

Goldsmith, H. L., and V. T. Turitto. 1986. Rheological aspects of thrombosis and haemostasis: basic principles and applications. *Thromb. Haemost.* 55:415–435.

Gresele, P., J. Arnout, H. Deckmyn, and J. Vermylen. 1986. Mechanism of the antiplatelet action of dipyridamole in whole blood: modulation of adenosine concentration and activity. *Thromb. Haemost.* 55:12–18.

Gresele, P., C. Zoja, H. Deckmyn, J. Arnout, J. Vermylen, and M. Verstraete. 1983. Dipyridamole inhibits platelet aggregation in whole blood. *Thromb. Haemost.* 50:852–856.

Harker, L. A., and R. A. Kadatz. 1983. Mechanism of action of dipyridamole. *Thromb. Res.* 4(Suppl):39–46.

Ikeda, Y., et al. 1991. The role of von Willebrand factor and fibrinogen in platelet aggregation under varying shear stress. *J. Clin. Invest.* 87: 1234–1240.

Jeffery, G. B. 1922. On the motion of ellipsoidal particles immersed in a viscous fluid. *Proc. R. Soc. (Lond.)* A102:162–179.

Jen, C. J., and L. V. McIntire. 1984. Characteristics of shear-induced aggregation in whole blood. *J. Lab. Clin. Med.* 103:115–124.

Karino, T., and H. L. Goldsmith. 1979. Adhesion of human platelets to collagen on the walls distal to a tubular expansion. *Microvasc. Res.* 17:238–262.

Manley, R. St. J., and S. G. Mason. 1952. Particle motions in sheared suspensions. II. Collisions of uniform spheres. *J. Colloid Sci.* 7:354–369.

Milton, J. G., and M. M. Frojmovic. 1994. Adrenaline and adenosine diphosphate-induced platelet aggregation require shape change. *J. Lab. Clin. Med.* 104:805–815.

Parker, J. C. 1970. Metabolism of external adenine nucleotides by human red blood cells. *Am. J. Physiol.* 218:1568–1574.

Saniabadi, A. R., G. D. O. Lowe, J. C. Barbenel, and C. D. Forbes. 1984. A comparison of spontaneous platelet aggregation in whole blood with platelet rich plasma: additional evidence for the role of ADP. *Thromb. Haemost.* 51:115–118.

Saniabadi, A. R., G. D. Lowe, J. C. Barbenel, and C. D. Forbes. 1985. Further studies on the role of red blood cells in spontaneous platelet aggregation. *Thromb. Res.* 38:225–232.

Saniabadi, A. R., G. D. Lowe, J. C. Barbenel, and C. D. Forbes. 1987. Effect of dipyridamole on spontaneous platelet aggregation in whole blood decreases with the time after venipuncture: evidence for the role of ADP. *Thromb. Haemost.* 58:744–748.

Saniabadi, A. R., R. H. Tomiak, G. D. Lowe, J. C. Barbenel, and C. D. Forbes. 1989. Dipyridamole inhibits red cell-induced platelet activation. *Atherosclerosis.* 76:149–154.

Skoza, L., M. B. Zucker, Z. Jerushalmy, and R. Grant. 1967. Kinetic studies of aggregation induced by adenosine diphosphate and its inhibition by chelating agents, guanido compounds, and adenosine. *Thromb. Diath. Haemorrh.* 18:713–725.

Smoluchowski, M. von. 1917. Versuch einer mathematischen Theorie der Koagulationskinetik kolloider Lösungen. *Z. Physik. Chem.* 92: 129–188.

Sung, P.-L., M. M. Frojmovic, T. E. O'Toole, E. F. Plow, J. C. Loftus, and M. Ginsberg. 1993. Determination of adhesion force between single cell pairs generated by activated GpIIb-IIIa receptors. *Blood.* 81:419–423.

Takamura, K., T. G. M. van de Ven, and S. G. Mason. The microrheology of colloidal dispersions. XI. Measured effects of Brownian motion on the rotation of doublets of spheres in shear flow. *J. Colloid Interface Sci.* 82:384–393, 1981.

Tangelder, G. J., H. C. Teirlinck, D. W. Slaaf, and R. S. Reneman. 1985. Distribution of blood platelets flowing in arterioles. *Am. J. Physiol.* 248:H318–H323.

Tha, S. P., J. Shuster, and H. L. Goldsmith. 1986. Interaction forces between red cells agglutinated by antibody. II. Measurement of hydrodynamic force of breakup. *Biophys. J.* 50:1117–1126.

Turitto, V. T., A. M. Benis, and E. F. Leonard. 1972. Platelet diffusion in flowing blood. *Ind. Eng. Chem. Fundam.* 11:216–223.

Turitto, V. T., and Baumgartner, H. R. 1975. Platelet interaction with subendothelium in a perfusion system: physical role of red blood cells. *Microvasc. Res.* 9:335–344.

van de Ven, T. G. M., K. Takamura, and S. G. Mason. The microrheology of colloidal dispersions. X. Rotations of spheroids at high Brenner numbers. *J. Colloid Interface Sci.* 82:373–383, 1981.

Wakiya, S. 1971. Slow motion in shear flow of a doublet of two spheres in contact. *J. Phys. Soc. Jpn.* 31:1581–1587. (errata, 1972, 33:278).